Monthly Notices
of the
ROYAL ASTRONOMICAL SOCIETY

Mon. Not. R. Astron. Soc. **404,** 265–274 (2010) doi:10.1111/j.1365-2966.2010.16281.x

Interstellar extinction and polarization – a spheroidal dust grain approach perspective

H. K. Das,[1⋆] N. V. Voshchinnikov[2⋆] and V. B. Il'in[2,3⋆]

[1]*IUCAA, Post Bag 4, Ganeshkhind, Pune 411 007, India*
[2]*Sobolev Astronomical Institute, St Petersburg University, St Petersburg 198504, Russia*
[3]*Main (Pulkovo) Astronomical Observatory, St Petersburg 196140, Russia*

Accepted 2009 December 30. Received 2009 December 16; in original form 2009 November 20

ABSTRACT

We extend and investigate the spheroidal model of interstellar dust grains used to simultaneously interpret the observed interstellar extinction and polarization curves. We compare our model with similar models recently suggested by other authors, study its properties and apply it to fit the normalized extinction $A(\lambda)/A_V$ and the polarizing efficiency $P(\lambda)/A(\lambda)$ measured in the near-infrared to far-ultraviolet region for several stars seen through one large cloud. We conclude that the model parameter Ω being the angle between the line of sight and the magnetic field direction can be more or less reliably determined from comparison of the theory and observations. This opens a way to study the spatial structure of interstellar magnetic fields by using multiwavelength photometric and polarimetric observations.

Key words: polarization – ISM: clouds – dust, extinction.

1 INTRODUCTION

Modelling of the wavelength dependencies of interstellar extinction $A(\lambda)$ and polarization $P(\lambda)$ along with analysis of infrared (IR) bands is the main source of information about the properties of interstellar grains (Draine 2003; Whittet 2003; Voshchinnikov 2004).

Extinction data were often used to constrain the size distribution of carbonaceous and silicate bare grains (e.g. Mathis, Rumpl & Nordsieck 1977; Zubko, Krełowski & Wegner 1996; Weingartner & Draine 2001). These data were also modelled with composite particles (Vaidya et al. 2001; Voshchinnikov et al. 2006; Iatì et al. 2008). In all these studies the grains were assumed to be spherical, i.e. their shape was not involved.

To get information about the grain shapes as well as the ambient magnetic fields, one needs to consider interstellar polarization. Interpretation of its wavelength dependence includes calculations of the extinction cross-sections of rotating partially aligned nonspherical particles. In early studies (e.g. Hong & Greenberg 1980; Voshchinnikov 1989), an unphysical model of infinitely long cylinders was applied.[1] More realistic is the spheroidal model of grains with the shape of these axisymmetric particles being characterized by the only parameter – the ratio of the major to minor semi-axis a/b. The optical properties of spheroids have long been of interest (e.g. Martin 1978; Rogers & Martin 1979; Onaka 1980; Draine & Lee 1984; Voshchinnikov & Farafonov 1993; Kim & Martin 1995). The growth of such grains in the interstellar medium (ISM) has been discussed by Stark, Potts & Diver (2006), their absorption and scattering properties (in the Rayleigh limit) by Min et al. (2006) and mineralogy by Li, Zhao & Li (2007).

Over the past decade spheroids have found wide applications in studies of optics of cometary dust – Das & Sen (2006), Moreno et al. (2007), circumstellar dust – Wolf, Voshchinnikov & Henning (2002), interplanetary dust – Lasue et al. (2007). Greenberg & Li (1996) used prolate spheroids and Lee & Draine (1985), Hildebrand & Dragovan (1995) oblate ones to interpret the silicate and ice polarization features of the Becklin–Neugebauer (BN) object. Draine & Allaf-Akbari (2006) predicted haloes due to X-ray scattering by oblate particles, detection of which would serve as a test for dust models.

The spheroidal model of cosmic dust grains is particularly promising for interpretation of the interstellar polarization and extinction data. A detailed review of early works on the subject can be found in Voshchinnikov (2004), so we consider recent applications of the model. Gupta et al. (2005) well reproduced the average Galactic extinction curve in the region 0.3–9.5 μm^{-1} with silicate and graphite oblate spheroidal ($a/b = 1.33$) particles rotating in a plane and having the size distribution $n(r_V) \propto r_V^{-3.5}$ with $r_V = 0.005$–0.25 μm where r_V is the radius of a volume equivalent sphere. They found that the shape of grains did not affect the abundance problem, but essentially changed the polarization efficiency factors at different particle orientation angles. It should be noted that interpretation of the extinction data alone is usually made within the spherical model of dust grains (see for details the recent review of Draine 2009). Draine & Allaf-Akbari (2006) and Draine & Fraisse (2009) fitted both the average Galactic extinction and polarization curves

⋆E-mail: hkdas@iucaa.ernet.in (HKD); nvv@astro.spbu.ru (NVV); ilin55@yandex.ru (VBI)

[1]Li & Greenberg (1997) also considered finite cylinders for modelling interstellar extinction and polarization.

in the range 0.4–9.5 μm^{-1} applying picket-fence oriented silicate and graphite oblate spheroids with the aspect ratio in the interval $a/b = 1$–2 with specific size distributions. The grain alignment degree was size dependent and showed a sharp increase at $r_V \sim 0.1$ μm. Voshchinnikov & Das (2008, hereafter VD08) studied the wavelength dependence of the ratio of the linear polarization degree to extinction (so called polarizing efficiency) from the ultraviolet (UV) to near-IR (NIR). They found that the wavelength dependence of $P(\lambda)/A(\lambda)$ was mainly determined by the particle composition and size whereas the absolute values of this ratio depended on the particle shape, degree and direction of alignment.

In this paper, we investigate further advantages of the spheroidal approach to interstellar grains. In contrast to other works, we calculate the optical properties of spheroids of all sizes exactly even at far-UV wavelengths, consider ensembles of particles with various degree and direction of alignment, compare different approaches to extinction and polarization curve modelling, treat the observational data in a new way (the wavelength dependence of the polarizing efficiency is fitted instead of the polarization curve), apply the theory to observational data for concrete stars, and discuss a possibility to determine the direction of interstellar magnetic fields from the data. In Section 2, we describe details of our model and compare it with the models used earlier. In Section 3, the results obtained from our model are compared with observations of seven stars for which the line of sight intersects one main cloud, keeping in view that 'mean extinction curves as well as mean total-to-selective extinction ratios are possibly averaged over several interstellar clouds of possibly different physical parameters' (Krełowski 1989). Section 4 contains our conclusions.

2 THEORY

Our modelling is based on the simple standard assumptions concerning dust grain materials, size distribution, shape and alignment. Homogeneous spheroids considered are characterized by their type (prolate or oblate), the aspect ratio *a*/*b* and a size parameter. As the latter we choose the radius r_V of a sphere whose volume is equal to that of a non-spherical particle, i.e. $r_V^3 = ab^2$ for prolate spheroids and $r_V^3 = a^2 b$ for oblate ones.

2.1 Dust grain materials

Interstellar dust mainly consists of five heavy elements: C, O, Mg, Si and Fe, which are locked in carbonaceous and silicate particles (Jones 2000; Draine 2009). We consider submicron grains from amorphous carbon (AC1) and amorphous silicate (astronomical silicate, astrosil). In order to reproduce the 2175 Å absorption feature small graphite spheres with radius $r_{gra} = 0.02$ μm are also involved.[2] The optical constants of the materials are taken from Rouleau & Martin (1991) and Laor & Draine (1993).

2.2 Size distribution

Interpretation of the interstellar extinction is usually aimed at reconstruction of the dust grain size distribution consistent with the cosmic abundances and some other constraints (see discussion in Voshchinnikov 2004).

[2]Note that graphite is not the only material considered as the carrier of the 2175 Å absorption feature (see, e.g. Li et al. 2008)

We choose a power-law size distribution,

$$n(r_V) \propto r_V^{-q}\,, \tag{1}$$

which was derived by Mathis et al. (1977) (see also Draine & Lee 1984) from minimization of χ^2-statistic. The distribution has three parameters: the lower ($r_{V,\min}$) and upper ($r_{V,\max}$) limits and the power index q. It was widely used in modelling of interstellar extinction and radiative transfer in dusty objects. The average Galactic extinction curve can be reproduced with the so-called standard Mathis, Rumpl & Nordsieck (MRN) mixture – an ensemble of carbonaceous (graphite) and silicate spheres (in nearly equal proportions) with the parameters: $q = 3.5$, $r_{V,\min} \approx 0.005$ μm and $r_{V,\max} \approx 0.25$ μm.

2.3 Cross-section averaging

Let us consider non-polarized light passing through a cloud that contains three populations of grains: rotating spheroids from amorphous silicate (Si), amorphous carbon (C) and graphite (gra) spheres. For a line of sight, extinction (in stellar magnitudes) and linear polarization (in per cent) produced by the cloud can be written as

$$A(\lambda) = 1.086 N_{\rm d} \langle C_{\rm ext}\rangle_\lambda\,, \qquad P(\lambda) = N_{\rm d}\langle C_{\rm pol}\rangle_\lambda 100\,\text{per cent}\,. \tag{2}$$

Here, $N_{\rm d} = N_{\rm C} + N_{\rm Si} + N_{\rm gra}$ is the total dust grain column density, $\langle C_{\rm ext}\rangle_\lambda$ and $\langle C_{\rm pol}\rangle_\lambda$ are the extinction and polarization cross-sections, respectively, averaged over the grain populations, i.e.

$$\langle C_{\rm ext}\rangle_\lambda = \mathcal{K}_{\rm C}\overline{C}_{\rm ext,C}(\lambda) + \mathcal{K}_{\rm Si}\overline{C}_{\rm ext,Si}(\lambda) + \mathcal{K}_{\rm gra}C_{\rm ext,gra}(\lambda)\,, \tag{3}$$

$$\langle C_{\rm pol}\rangle_\lambda = \mathcal{K}_{\rm C}\overline{C}_{\rm pol,C}(\lambda) + \mathcal{K}_{\rm Si}\overline{C}_{\rm pol,Si}(\lambda)\,, \tag{4}$$

where $C_{\rm ext,gra}(\lambda) = \pi r_{\rm gra}^2 Q_{\rm ext,gra}(\lambda)$ and $\mathcal{K}_i = N_i/N_{\rm d}$ (i = C, Si, gra) is the relative column density of the ith population. It is evident that

$$\mathcal{K}_{\rm C} + \mathcal{K}_{\rm Si} + \mathcal{K}_{\rm gra} = 1.$$

The values of $\overline{C}_{{\rm ext},\,j}$ and $\overline{C}_{{\rm pol},\,j}$ (j = C, Si) are obtained by averaging of the cross-sections over the size distribution and grain orientations (Hong & Greenberg 1980; Voshchinnikov 1989),

$$\overline{C}_{{\rm ext},\,j}(\lambda) = \left(\frac{2}{\pi}\right)^2 \int_{r_{V,\min,\,j}}^{r_{V,\max,\,j}} \int_0^{\pi/2}\int_0^{\pi/2}\int_0^{\pi/2} \pi r_{V,\,j}^2\, Q_{{\rm ext},\,j}(\lambda) \times n_j(r_V)\, f(\xi,\beta)\,{\rm d}\varphi\,{\rm d}\omega\,{\rm d}\beta\,{\rm d}r_V\,, \tag{5}$$

$$\overline{C}_{{\rm pol},\,j}(\lambda) = \frac{2}{\pi^2} \int_{r_{V,\min,\,j}}^{r_{V,\max,\,j}} \int_0^{\pi/2}\int_0^{\pi}\int_0^{\pi/2} \pi r_{V,\,j}^2\, Q_{{\rm pol},\,j}(\lambda) \times n_j(r_V)\, f(\xi,\beta)\,\cos 2\psi\,{\rm d}\varphi\,{\rm d}\omega\,{\rm d}\beta\,{\rm d}r_V\,. \tag{6}$$

Here, β is the precession-cone angle for the angular momentum J which spins around the direction of the magnetic field B, φ the spin angle, ω the precession angle (see Fig. 1). The quantities $Q_{\rm ext} = (Q_{\rm ext}^{\rm TM} + Q_{\rm ext}^{\rm TE})/2$ and $Q_{\rm pol} = (Q_{\rm ext}^{\rm TM} - Q_{\rm ext}^{\rm TE})/2$ are the extinction and polarization efficiency factors for non-polarized incident radiation (Voshchinnikov & Farafonov 1993),

$$\cos 2\psi = \begin{cases} \cos 2\Phi \left[\frac{2\cos^2\varphi\cos^2\theta}{1-\cos^2\varphi\sin^2\theta} - 1\right], & \text{prolate} \\ \cos 2\Phi, & \text{oblate,} \end{cases} \tag{7}$$

and

$$\cos\theta = \cos\Omega\cos\beta + \sin\Omega\sin\beta\cos\omega, \tag{8}$$

$$\cos 2\Phi = \left[\frac{2\sin^2\beta\sin^2\omega}{\sin^2\theta} - 1\right], \tag{9}$$

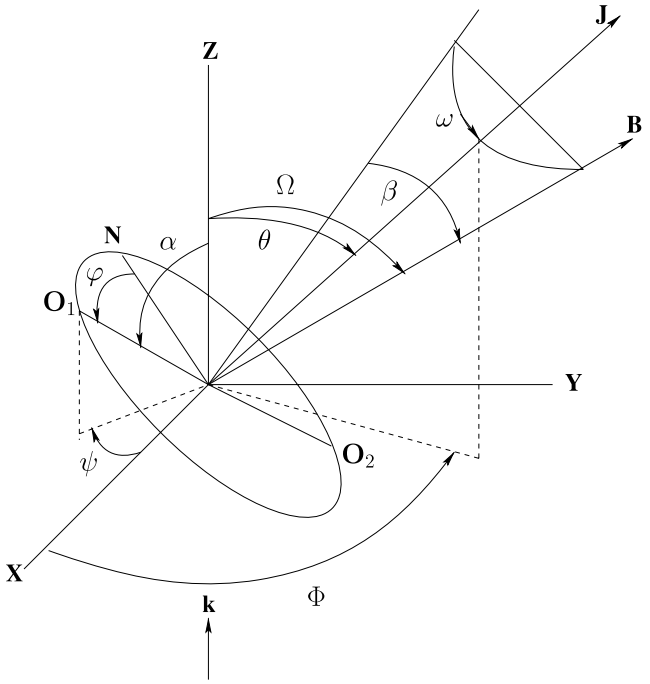

Figure 1. Geometrical configuration of a spinning and wobbling prolate spheroidal grain. The major (symmetry) axis of the particle O_1O_2 is situated in the spinning plane NO_1O_2 which is perpendicular to the angular momentum J. The direction of light propagation k is parallel to the Z-axis and makes the angle α with the particle symmetry axis.

$$\cos\alpha = \begin{cases} \sin\theta\cos\varphi, & \text{prolate} \\ \sqrt{1-\sin^2\theta\cos^2\varphi}, & \text{oblate.} \end{cases} \tag{10}$$

Here, Ω is the angle between the line of sight and the magnetic field direction ($0^\circ \le \Omega \le 90^\circ$). The value $\Omega = 90^\circ$ corresponds to the case when the particle rotation plane contains the light propagation vector $\boldsymbol{k}$, which gives the maximum degree of linear polarization. For $\Omega = 0^\circ$, the light falls perpendicular to the particle rotation plane and from symmetry reasons the net degree of polarization produced is zero.

The efficiency factors were calculated by using a solution to the light scattering problem for a homogeneous spheroid obtained by the method of separation of variables in spheroidal coordinates (Voshchinnikov & Farafonov 1993) and a modern approach to computations of spheroidal wave functions (Voshchinnikov & Farafonov 2003). In contrast to all works where the spheroidal model was recently applied (Gupta et al. 2005; Draine 2009; Draine & Fraisse 2009), we computed the optical properties of the particles of all sizes exactly even in the far-UV spectral region.

2.4 Grain alignment

Interstellar non-spherical grains should be partially aligned. The 'picket fence' or perfect rotating alignment often used in modelling of polarization (e.g. Kim & Martin 1995; Draine & Fraisse 2009) is a crude approximation giving a too high polarizing efficiency in comparison with the empirical upper limit (e.g. Greenberg 1978)

$$P_{\max}/A_V \lesssim 3\,\text{per cent/mag}.$$

Although the theory of grain alignment is actively discussed (Lazarian 2007) it still has little practical significance. Therefore, we consider the classical alignment mechanism – so-called imperfect Davis–Greenstein (DG) orientation (Davis & Greenstein 1951). The imperfect DG mechanism is described by the function $f(\xi,\beta)$ depending on the alignment parameter ξ and the precession angle β (Hong & Greenberg 1980; Voshchinnikov 1989),

$$f(\xi,\beta) = \frac{\xi\sin\beta}{(\xi^2\cos^2\beta+\sin^2\beta)^{3/2}}. \tag{11}$$

The parameter ξ depends on the particle size r_V, the imaginary part of the grain magnetic susceptibility $\chi'' = \varkappa\omega_{\rm d}/T_{\rm d}$, where $\omega_{\rm d}$ is the angular velocity of a grain and $\varkappa = 2.5\times10^{-12}$ (Davis & Greenstein 1951), gas density $n_{\rm H}$, the strength of magnetic field B, and temperatures of dust $T_{\rm d}$ and gas $T_{\rm g}$. By introducing a parameter

$$\delta_0 = 8.23\times10^{23}\frac{\varkappa B^2}{n_{\rm H}T_{\rm g}^{1/2}T_{\rm d}}\ \mu\text{m}, \tag{12}$$

one can get

$$\xi^2 = \frac{r_V+\delta_0(T_{\rm d}/T_{\rm g})}{r_V+\delta_0}. \tag{13}$$

We assume that carbon and silicate grains have similar alignment but different size distributions. Thus, our model has 10 main parameters: $r_{V,\min}$, $r_{V,\max}$ and q for carbon and silicate grains, relative density for carbon ($\mathcal{K}_{\rm C}$) and silicate ($\mathcal{K}_{\rm Si}$) grains, degree (δ_0) and direction (Ω) of grain alignment.

2.5 Comparison with other models

There were just a few approaches to simultaneous modelling of the wavelength dependencies of interstellar extinction and linear polarization. In most of the papers where an imperfect alignment of grains was involved (along with a power-law size distribution), the authors derived that particles with $r_V \lesssim 0.1$ μm should be poorly (randomly) oriented while those with $r_V \gtrsim 0.1$ μm should be nearly perfectly aligned (e.g. Kim & Martin 1995; Draine & Fraisse 2009). Some physical grounds for such alignment of interstellar grains come e.g. from Mathis (1986) and Goodman & Whittet (1995), Martin (1995).

As the actual composition of carbonaceous grains in the ISM is still unknown (Draine & Fraisse 2009), in interstellar dust modelling one often considered large (sub-micron) graphite grains instead of amorphous carbon ones. As polarization produced by such graphite spheroids may be to a certain extent peculiar, the carbonaceous grains were often assumed to be either spherical or randomly aligned (e.g. Mathis 1986; Draine & Fraisse 2009).

To compare these approaches with our one, we have made some calculations for three additional models:

model A1– imperfectly DG-aligned silicate and graphite spheroids;

model A2– imperfectly DG-aligned silicate spheroids and randomly oriented amorphous carbon spheroids;

model A3– silicate and amorphous carbon spheroids with randomly oriented small particle and perfectly DG-aligned large particle.

The grain size distributions and the population of small graphite particles are not varied, i.e. they are the same as in our basic model described in Sections 2.1–2.4.

When considering graphite spheroids in the A1 model, we use the standard 2/3–1/3 approximation which gives reasonably accurate results (Draine & Malhotra 1993). The orientation function for amorphous carbon grains in the A2 model is $f(\beta) = \sin\beta$. In the

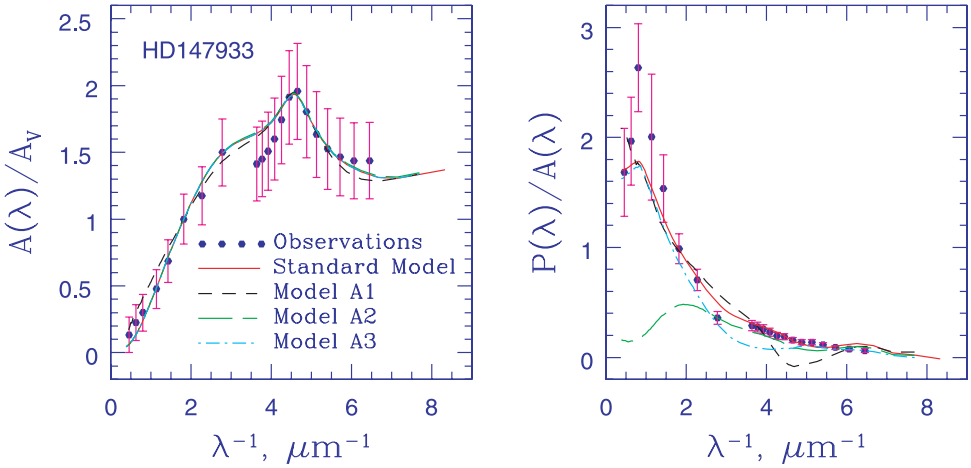

Figure 2. Normalized extinction (left-hand panel) and polarizing efficiency (right-hand panel) for our basic model and three additional models with graphite spheroids (A1); randomly oriented amorphous carbon spheroids (A2); small randomly oriented silicate and amorphous carbon spheroids (A3) (see the text for mode details). Oblate spheroids with $a/b = 3$ and $\Omega = 33°$, for other parameters see the last line in Table 3. Observational data for HD 147933.

A3 model, this function is size dependent

$$f(\beta, r_V) = \begin{cases} \sin\beta & \text{for } r_V \le r_{V,\rm cut} \\ \delta(\beta) & \text{for } r_V > r_{V,\rm cut} \end{cases}, \qquad (14)$$

where $\delta(\beta)$ is the Dirac delta function, $r_{V,\rm cut}$ a cut-off parameter.

So, we assume that all particles whose volume is smaller than that of a sphere with the radius $r_{V,\rm cut}$ are randomly oriented, while other particles have perfect rotation alignment, i.e. their angular moment vectors are parallel to the magnetic field direction. In our calculations, we choose $r_{V,\rm cut}$ to be 0.11 μm (cf. Draine & Fraisse 2009).

Some results obtained with the models considered are presented in Fig. 2; the fitting procedure used is described in the next section. We see that all models can give very similar extinction curves that well fit the observational data. Only the A1 model with large graphite particles provides a curve that differs a bit from others. Certainly, the extinction data are not enough to constrain the models.

The model dependencies of polarizing efficiency shown in the right-hand panel of the figure vary in form. In particular, the model with randomly oriented carbonaceous particles produces too small a polarization in the visual and IR parts of the spectrum. Apparently, in this case, a better fit can be reached if one takes a more complex size distribution function or (and) increases the alignment efficiency of silicate grains. However, this complicates the model, therefore, we prefer our model having a small number of the parameters and simple assumptions.

3 COMPARISON WITH OBSERVATIONAL DATA

So far, most efforts in modelling of the optics of interstellar dust were directed at fitting of the average Galactic extinction curve (often with some additional constraints) by making use of spherical particles. Interpretation of the curves observed towards individual objects was very seldom done, and that of the extinction and polarization curves was done only for a few objects. Il'in (1987) applied the model of infinitely long coated cylinders with the imperfect DG-alignment to the interpretation of the wavelength dependence of interstellar extinction, linear and circular polarization for the star HD 204827 in the visual and IR parts of the spectrum. Kim & Martin (1994) used infinitely long cylinders with the perfect DG-alignment ($\Omega = 90°$) to interpret the data for HD 25443 and HD 197770. Infinitely long cylinders with a silicate core and organic refractory mantle were chosen by Li & Greenberg (1998) for the interpretation of the extinction and polarization curves for HD 210121. So, VD08 were the first to utilize the spheroidal model to consider both the extinction and polarization wavelength dependencies observed for two stars.

Table 1. Target stars.

Star	l	b	D (pc)	Sp	R_V	A_V
HD 24263	182.1	−34.9	171	B5V	3.44	0.72
HD 62542	255.9	−9.2	396	B5V	2.74	0.99
HD 99264	296.3	−10.5	266	B2.5V	3.15	0.85
HD 147165	351.3	+17.0	137	B1III	3.60	1.48
HD 147933	353.7	+17.7	118	B2.5V	4.41	2.07
HD 179406	28.2	−8.3	227	B3V	2.88	0.89
HD 197770	93.9	+9.0	943	B2V	2.77	1.61

3.1 Sample of objects

For application of our model, we chose stars seen through a single cloud with the extinction and polarization curves known in a wide wavelength region. Initially, preference was given to five stars (HD 24263, HD 62542, HD 99264, HD 147933 and HD 197770) with measured UV polarization (Anderson et al. 1996). These stars are not peculiar and not very distant. Later, two stars (HD 147165 and HD 179406) for which the polarization data in the visible were obtained by us were added to our sample.

In this paper, we discuss extinction and polarization of six stars (HD 24263, HD 99264, HD 147165, HD 147933, HD 179406 and HD 197770). Two objects (HD 62542 and HD 147933) were considered in our previous paper (VD08). Almost all the stars are not very far away from the galactic plane (Table 1) and are in dusty environments. One can assume that these stars are seen through single dust clouds as they have weak rotation angle of linear polarization (Anderson et al. 1996) and narrow symmetric sodium D_1 and D_2 lines (Zubko et al. 1996). A few comments on the stars should be made.

HD 24263 is a double star (the secondary is a B9 star) seen through a large cloud AG6 located between the Local Bubble and

Orion–Eridanus Super-bubble at a distance ∼150 pc and observed in Na I D and Ca II lines (Genova & Beckman 2003; Welsh, Sallmen & Jelinsky 2005). One also detects the molecules CH, CH^+ and CN in the line of sight (Penprase et al. 1990).

HD 99264 is located in the region of the Scorpio–Centaurus OB association and the Chamaeleon–Musca dark clouds (Platais, Kozhurina-Platais & van Leeuwen 1998; Corradi, Franko & Knude 2004). Consideration of high-resolution Na I D profiles and $uvby\beta$ photometry for over 60 nearby B stars allows Corradi et al. (2004) to conclude that interstellar gas and dust in this region are distributed in two extended sheet-like structures. The nearby feature located at the distance <60 pc provides the colour excess $E(b-y) \approx 0.05$ while the second feature at 120–150 pc has $E(b-y) \approx 0.2$.

HD 147165 (σ Sco) is a beta Cephei type pulsating variable and a spectroscopic binary with the secondary being a B1V star (North et al. 2007). It is a member of the Upper Scorpius subgroup within the Sco OB2 association related to the reflection nebula in the Ophiuchus cloud complex region (Mamajek 2008).

HD 147933 is a component of the well-studied binary star ρ Oph AB. High-resolution K I, Na I, Ca II observations show very complex profiles of atomic lines in its spectrum (Snow, Destree & Welty 2008). The star is associated with a strong reflection nebula and a significant amount of dust (and gas) is assumed to lie behind it.

HD 179406 (20 Aql) is a variable star behind a translucent cloud (Hanson, Snow & Black 1992; Dobashi et. al. 2005). Though the absorption and emission lines have at least three components, the dominant one is seen in most of the atomic and all molecular lines.

HD 197770 is an evolved spectroscopic eclipsing binary star with both components being B2III stars (Clayton 1996). The object is close to Cyg OB7 and Cep OB2 and probably lies on the edge of a star formation region including molecular clouds L1036 and L1049. It is associated with non-stellar *IRAS* sources (see for more details Gordon et al. 1998).

So, the clouds observed in the selected lines of sight look to be rather different and hence their dust grain ensemble parameters may also differ.

3.2 Observational data

Basic information on the selected stars is presented in Table 1. The distance D, colour excess $E(B-V)$, ratio of total extinction to the selective one R_V and extinction A_V for all stars except HD 24263 and 197770 are from Fitzpatrick & Massa (2007), with the data for these two stars being from Valencic, Clayton & Gordon (2004). The Morgan and Keenan (MK) spectral types were taken from the catalogue of stellar spectral classifications (Skiff 2009).

The photometric data in the standard visual–NIR bands were found in the general catalogue of photometric data (Mermilliod, Mermilliod & Hauck 1997) and recent papers referred to in the SIMBAD data base (see Table 2). When the *JHK* data were unavailable, the JHK_S values from the Two-Micron All-Sky Survey catalogue (Cutri et al. 2003) were used. When the IR data were absent, we applied with caution the data from the USNO B1 catalogue (Monet et al. 2003). To derive the interstellar extinction in the line of sight, the intrinsic colours from Straizys (1992) were utilized. The UV extinction parameters were taken from Valencic et al. (2004) and Fitzpatrick & Massa (2007).

Uncertainties of UV extinction are mainly a result of errors in R_V and A_V values. Note that typical relative errors of these quantities are 10–15 per cent (see, e.g. Valencic et al. 2004). An additional source of relatively large errors of extinction values in the visual and NIR regions is uncertainty of the intrinsic colours (cf. e.g. Bessell & Brett 1988; Straizys 1992; Ducati et al. 2001). So, relative errors of extinction for individual objects are rather large (see, e.g. Fig. 2).

Table 2 also contains references to the papers with polarimetric data. Additional polarimetric observations of HD 147165 and HD 179406 were performed by one of the authors (H. K. Das) in 2007 at a 2-m telescope of the Girawali Observatory (Pune, India). The IUCAA Faint Object Spectrograph and Camera (IFOSC) was used in the polarimetric mode. The polarization parameters were measured in 10 bands in the wavelength region about 0.37–0.60 μm and a standard package was applied for data analysis.

Note that for two stars (HD 62542 and HD 197770), far-UV extinction curves were derived from *International Ultraviolet Explorer* (*IUE*) and *The Far Ultraviolet Spectroscopic Explorer* (*FUSE*) observations by Sofia et al. (2005). For two stars (HD 147933 and HD 197770), the important polarization data in the *J, H* and *K* bands are also available (Wilking et al. 1980; Wilking, Lebofsky & Rieki 1982).

3.3 Fitting procedure and parameter variations

A general problem of dust optics modelling is in obtaining the absolute values of the model parameters. As has been noted many times (e.g. Greenberg 1978), similar extinction occurs when a product of the typical particle size $\langle r \rangle$ and the particle refractive index does not change, i.e.

$$\langle r \rangle \, |m-1| \approx \text{const}.$$

The average Galactic extinction curve was successfully reproduced using quite different mixtures of particles with exponential (Hong & Greenberg 1980), power-law (Mathis et al. 1977) and more complicated grain size distributions (Mathis 1996; Weingartner &

Table 2. Photometric and polarimetric data sources.

Star	Photometry[a]	Polarimetry[b]
HD 24263	V04 (UV); M97 (*UBV*); M03 (RI); L05 (*JHKL*)	A96 (UV and vis–NIR)
HD 62542	S05 (far-UV); F07 (UV); M97 (*BV*); M03 (RI); C03 (JHK_S)	A96 (UV & vis–NIR)
HD 99264	F07 (UV); M97 (*UBVRI*); C03 (JHK_S)	A96 (UV and vis); S69 (*UBV*)
HD 147165	V04 (UV); W02 (*UBVRIJHKLM*)	This work (vis); C66 (vis–NIR)
HD 147933	F07 (UV); M97 (*UBVRI*); C03 (JHK_S)	A96 (UV–NIR)
HD 179406	V04 (UV); W02 (*UBVJHKL*); M03 (RI)	This work (vis)
HD 197770	S05 (far-UV); V04 (UV); M97 (*UBV*); M03 (RI); C03 (JHK_S)	A96 (UV–NIR)

[a]M97 is for Mermilliod et al. (1997), W02 for Wegner (2002), C03 for Cutri et al. (2003), M03 for Monet et al. (2003), V04 for Valencic et al. (2004), L05 for Larson & Whittet (2005), S05 for Sofia et al. (2005), F07 for Fitzpatrick & Massa (2007).
[b]C66 is for Coyne & Gehrels (1966), S69 for Serkowski & Robertson (1969), A96 for Anderson et al. (1996).

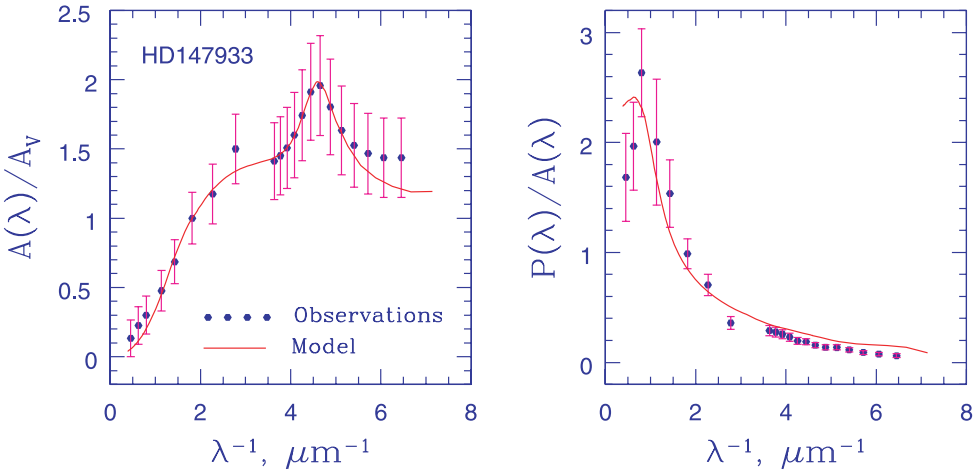

Figure 3. Comparison of the normalized extinction (left-hand panel) and the polarizing efficiency (right-hand panel) observed for HD 147933 with results of modelling. The solid curves show the case of prolate ($a/b = 3$) spheroids having a power-law size distribution. Other model parameters are given in Table 3.

Draine 2001). Effects of variations of the distribution parameters (e.g. $r_{V,\min}$, $r_{V,\max}$, q for a power-law distribution) on extinction are well studied for spheres (see, for example, Voshchinnikov & Il'in 1993).

Joint modelling of interstellar extinction and polarization adds at least one parameter – particle shape – to the model. In the case of spheroids, the particle shape is defined by the spheroid's aspect ratio *a*/*b*. Besides this, we can consider prolate ('cigars') and oblate ('pancakes') spheroids. If such particles are imperfectly oriented, the alignment parameters (in our case, δ_0 and Ω) very weakly affect extinction. Note that the normalized extinction A_λ/A_V essentially changes in the UV region when *a*/*b* varies (see fig. 3 in VD08).

In order to analyse importance of the model parameters, we reproduced the observational data available for HD 147933 with different particles. Some results are shown in Figs 2 and 3 (see also fig. 8 in VD08); the parameters of the fits are given in Table 3. Note that in VD08, the fitting was simply 'chi-by-eye' while in this paper we apply minimization of χ^2.

The fitting approach used included two steps: (i) finding of the size distribution parameters and the relative column densities $\mathcal{K}_i$ from approximation of the extinction data using particles of given shape, and (ii) a more accurate determination of the alignment parameters δ_0 and Ω from fitting of the wavelength dependence of polarizing efficiency $P(\lambda)/A(\lambda)$.

It is interesting that by varying the parameters $r_{V,\min}$, $r_{V,\max}$ and q and the relative density of carbon ($\mathcal{K}_C$) and silicate ($\mathcal{K}_{Si}$) grains one can reproduce the observational data with prolate as well as oblate particles of different aspect ratios. Note that after fixing the particle type (prolate/oblate) and *a*/*b*, one can estimate only the values of $\mathcal{K}_C$, $\mathcal{K}_{Si}$, $r_{V,\min}$ and q as the extinction and polarization curves are little affected by variation of $r_{V,\max}$.

The alignment degree for three models presented in Table 3 is found to be slightly larger than the standard interstellar value ($\delta_0 \approx 0.2\,\mu$m; Voshchinnikov 1989). This can be a result of enhanced magnetic fields in the interstellar cloud near ρ Oph to which HD 147933 is related. The most exciting conclusion of our modelling is a close coincidence of the magnetic field directions – the values of Ω for various fits differ less than 10°. We suggest that this model parameter can be more or less reliably determined from such modelling.

Possibly, a better coincidence of the theory with the observations could be obtained if we consider different alignment parameters for silicate and carbonaceous grains. Certainly, consideration of non-aligned carbonaceous grains cannot be ruled out (Li & Greenberg 2002; Chiar et al. 2005; see, however, Fig. 2).

3.4 Fitting results and discussion

The normalized extinction $A(\lambda)/A_V$ and the polarizing efficiency $P(\lambda)/A(\lambda)$ were calculated with the theory of Section 2 and compared with the observational data available for the stars mentioned in Section 3.1. The results of this comparison are plotted in Figs 3–4 (see also fig. 9 in VD08 for HD 62542) with the parameters of the fits being presented in Table 4. We start with comments on the individual objects and then make general conclusions.

HD 62542. The UV extinction curve has a very broad and weak 2175 Å bump and a steep far-UV rise (Snow & McCall 2006). Our model suggests that the major part of grains are small carbon particles with a very narrow size distribution.

HD 99264. The extinction curve for it is characterized by R_V of about three (Fitzpatrick & Massa 2007); the UV extinction curve

Table 3. Modelling results for HD 147933.

Amorphous carbon				Astrosil				Graphite	shape;			χ^2	
$\mathcal{K}_C$	$r_{V,\min}$[a]	$r_{V,\max}$	q	$\mathcal{K}_{Si}$	$r_{V,\min}$	$r_{V,\max}$	q	$\mathcal{K}_{gra}$	*a*/*b*	$\delta_0(\mu m)$	Ω (°)	A/A_V	P/A
0.24	0.03	0.15	1.5	0.73	0.08	0.25	1.5	0.03	pro; 5	0.5	35	1.04	24.6
0.54	0.10	0.20	2.0	0.40	0.01	0.25	1.3	0.06	pro; 3	0.3	42	0.19	8.2
0.50	0.10	0.25	2.0	0.47	0.07	0.20	2.0	0.03	obl; 3	0.3	33	0.19	2.2

[a] $r_{V,\min}$ and $r_{V,\max}$ are in μm.

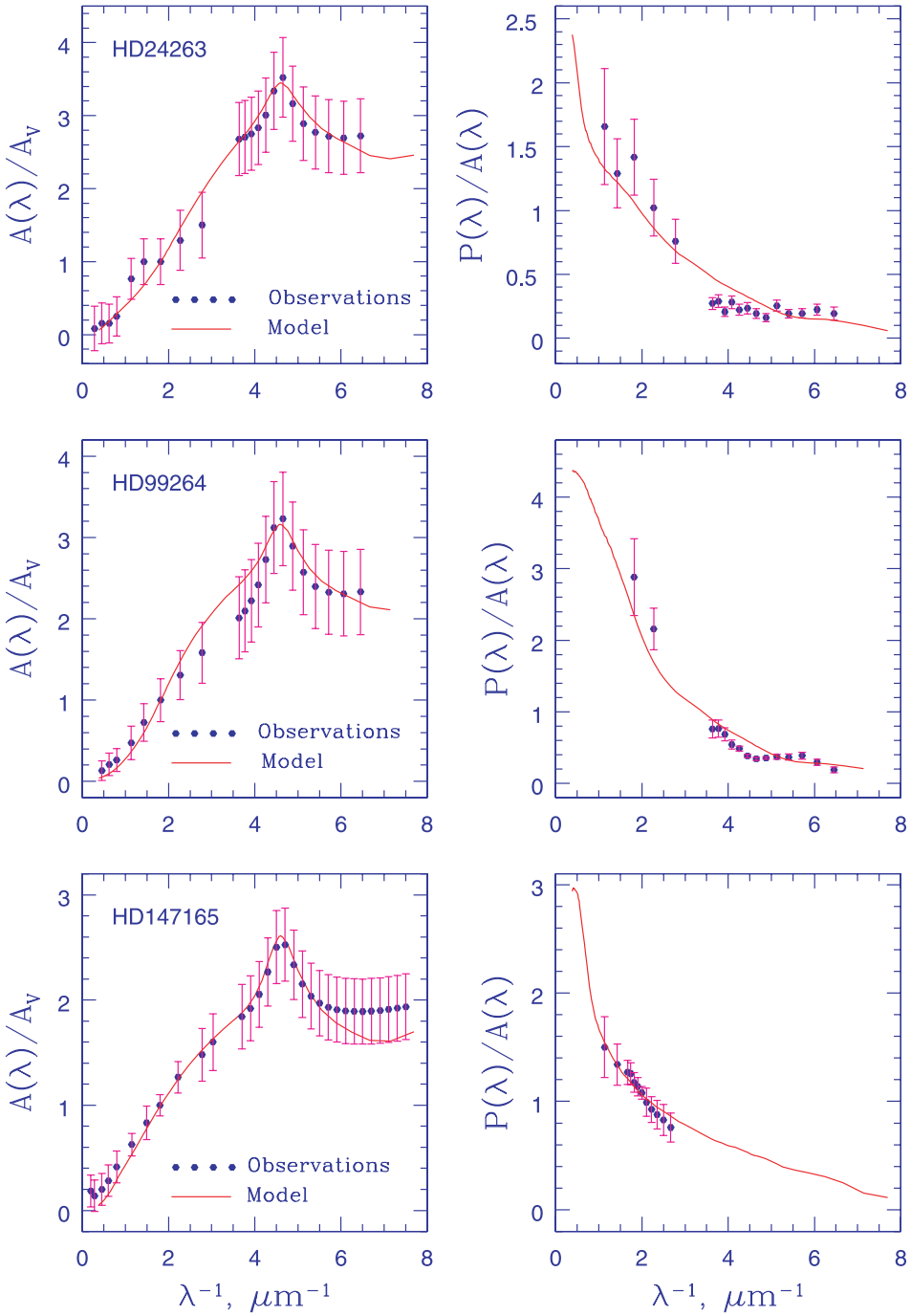

Figure 4. Comparison of observed and modelled normalized extinction (left-hand panel) and polarizing efficiency (right-hand panel) for five stars. The solid curves show results of calculations. The model parameters are given in Table 4.

is a bit 'shallow' but not anomalous (Carnochan 1986). The polarization in the UV region and the *UBV* bands is well described by a Serkowski curve with $\lambda_{max} = 0.55$ μm (Anderson et al. 1996; Martin, Clayton & Wolff 1999). So, we have the case close to the average Galactic curves, but certainly there are not enough polarization data for sound comparison.

HD 147165 and *HD 179406*. Extinction in these lines of sight along with element abundances were interpreted by Zubko et al. (1996) and Zubko, Krełowski & Wegner (1998) using rather wide size distributions of grains. These authors applied spherical particles of different materials as well as inhomogeneous particles, which makes impossible a direct comparison of their results with those obtained in our work.

HD 197770. For this star, the polarizing efficiency is maximal: it reaches $P/A = 3.7$ at the J band ($\lambda = 1.25$ μm). The polarization is enhanced in the region of the UV bump (super-Serkowski behaviour), but a strong UV bump in extinction results in no structure for the P/A curve (see insert in Fig. 4). Our model shows the largest fraction of graphite in the grain mixture for this star.

Thus, we have fitted the observational data using prolate or oblate spheroids with $a/b = 2$ or 3 and intermediate values of the

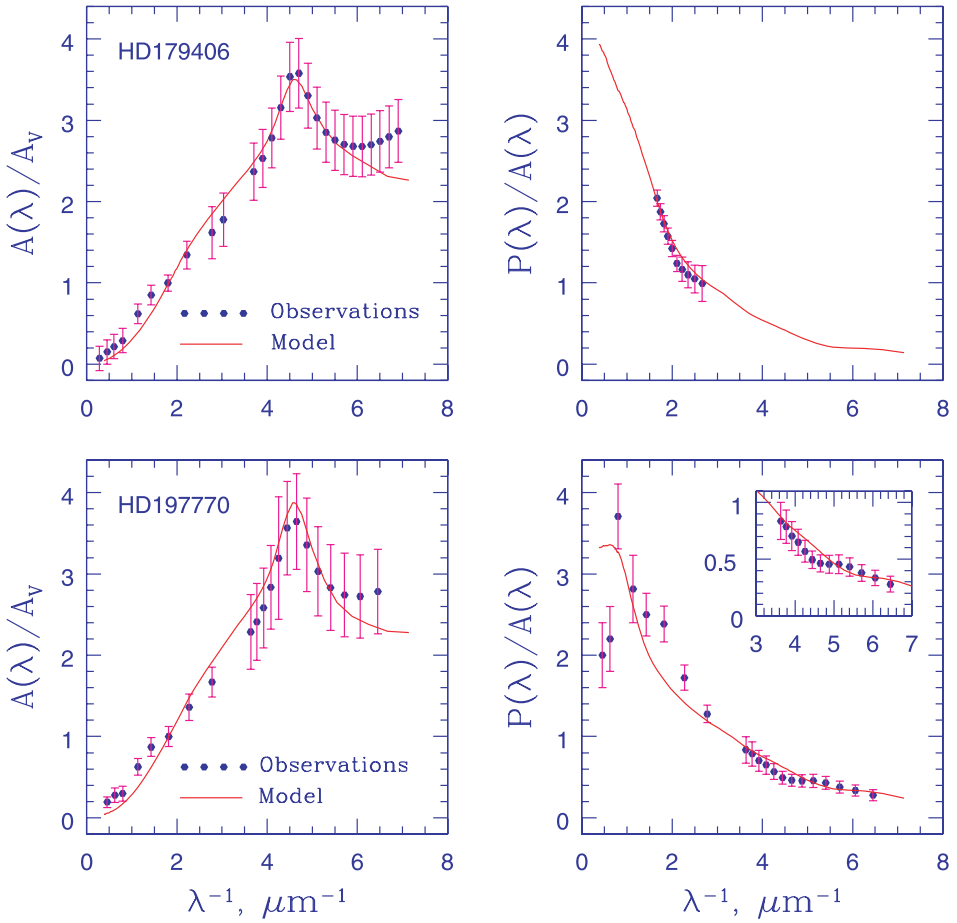

Figure 4 – *continued*

Table 4. Modelling results.

Star	Amorphous carbon $\mathcal{K}_C$	$r_{V,\min}$[a]	$r_{V,\max}$	q	Astrosil $\mathcal{K}_{Si}$	$r_{V,\min}$	$r_{V,\max}$	q	Graphite $\mathcal{K}_{gra}$	shape; a/b	$\delta_0(\mu m)$	Ω (°)
HD 24263	0.48	0.08	0.40	3.5	0.47	0.04	0.15	2.1	0.05	Pro; 2	0.3	60
HD 62542	0.85	0.07	0.10	2.7	0.10	0.005	0.25	2.7	0.05	Pro; 2	0.5	40
HD 99264	0.44	0.09	0.30	6.0	0.50	0.04	0.18	2.0	0.06	Pro; 3	0.5	50
HD 147165	0.49	0.06	0.30	2.2	0.44	0.04	0.20	2.2	0.07	Pro; 2	0.5	54
HD 147933	0.50	0.10	0.25	2.0	0.47	0.07	0.20	2.0	0.03	Obl; 3	0.3	33
HD 179406	0.45	0.10	0.40	6.0	0.47	0.04	0.18	2.5	0.08	Pro; 3	0.5	49
HD 197770	0.43	0.05	0.20	2.8	0.46	0.01	0.17	1.3	0.11	Pro; 3	0.5	42

[a] $r_{V,\min}$ and $r_{V,\max}$ are in μm.

alignment parameter $\delta_0 = 0.3$–0.5 μm. Contributions of carbonaceous and silicate grains to extinction and polarization are nearly equal excluding the case of HD 62542 for which extinction is very peculiar. The contribution of small graphite particles to extinction usually is less than 10 per cent. The parameters of the size distributions for silicate and amorphous carbon grains differ from the standard MRN mixture (see Section 2.2). As usual, very small particles with $r_{V,\min} \lesssim 0.01$ μm are absent in the grain ensembles. Besides this, in many cases, the slope of the $n(r_V)$ dependence is less steep than that for the MRN mixture (i.e. $q < 3.5$).

The inclination of the magnetic field direction relative to the line of sight determined for all target stars lies in the interval $\Omega \approx 30°$–$60°$. These values of Ω are derived rather accurately because of a strong dependence of P/A on Ω (see figs 4 and 6 in VD08). The magnetic fields seem to be connected with local dust clouds in the directions to the selected stars. At the same time, the obtained values of Ω do not contradict the general pattern of the galactic magnetic field in the solar neighbourhood as found from pulsar measurements (Vallée 2004, 2008).

It should be noted that one usually assumed that small grains were badly oriented as the interstellar polarization degree decreases with a growing λ^{-1} in the UV region (Whittet 2003). However, for all the objects, we have fitted the observational data by using the simple size and orientation distributions with small particles being rather well aligned. To see that one should consider equations (11)–(13) and keep in mind that δ_0 is about 0.4 and the temperature ratio about 0.1. For $r_V \sim 0.06$ μm, this gives $\xi \sim 0.5$ when $\xi = 0$ corresponds to the perfect alignment while $\xi = 1$ means the random orientation.

4 CONCLUSIONS

We have extended the spheroidal model of interstellar dust by considering imperfectly dynamically aligned amorphous carbon and silicate prolate and oblate spheroids with a power-law size distribution and a small fraction of graphite spheres involved to explain the 2175 Å bump. Our model being as simple as possible was applied to fit the normalized extinction $A(\lambda)/A_V$ and the polarizing efficiency $P(\lambda)/A(\lambda)$ observed in the NIR to far-UV region.

In contrast to the earlier works, we exactly calculated the optical properties of spheroids, for the first time utilized their imperfect Davis–Greenstein alignment and applied the spheroidal model to fit the data obtained for individual stars instead of the commonly used average Galactic curves.

A comparison of our model with those recently suggested by other authors has demonstrated that the extinction data are well fitted by all the models while only our model allows one to satisfactorily fit the polarization data with simple size and orientation distributions. Contrary to other works, we find that the data can be well fitted with aligned carbonaceous and small silicate non-spherical grains.

Investigation of our model has shown that the only parameter that can be determined more or less accurately from observational data fitting is the direction of magnetic field relative to the line of sight. As the projection of the magnetic field on the sky plane is given by the positional angle of polarization ϑ, multiwavelength extinction and polarization observations can be used for the study of the spatial structure of interstellar magnetic fields.

Variations of the interstellar extinction and polarization curves for the considered stars can be interpreted by differences in the relative fractions of carbon and silicate grains and their size distributions in the clouds crossed by the lines of sight with the alignment parameter having intermediate values $\delta_0 = 0.3$–0.5 μm (for the particle aspect ratio $a/b = 2$–3). We assume that ambiguous results could be ruled out by considering dust phase abundances.

ACKNOWLEDGMENTS

One of the authors (HKD) is deeply indebted to the IUCAA's instrumentation and observatory team for their support and cooperation extended during the course of this work. The work was partly supported by the grants RFBR 07-02-00831, NTP 2.1.1/665 and NSh 1318.2008.2.

REFERENCES

Anderson C. M. et al., 1996, AJ, 112, 2726
Bessell M. S., Brett J. M., 1988, PASP, 100, 1134
Carnochan D. J., 1986, MNRAS, 219, 903
Chiar J. E. et al., 2005, in Adamson A., Aspin C., Davis C. J., Fujiyoshi T., eds, ASP Conf. Ser. Vol. 343, Astronomical Polarimetry: Current Status and Future Directions. Astron. Soc. Pac., San Francisco, p. 352
Clayton G. C., 1996, PASP, 108, 401
Corradi W. J. B., Franco G. A. P., Knude J., 2004, MNRAS, 347, 1065
Coyne G. V., Gehrels T., 1966, AJ, 71, 355
Cutri R. M. et al., 2003, 2MASS All-Sky Catalogue of Point Sources, Univ. Massachusetts and IPAC/California Institute of Technology. VizieR On-line Data Catalog
Das H. S., Sen A. K., 2006, A&A, 459, 271
Davis L., Greenstein J. L., 1951, ApJ, 114, 206
Davis J., Tuthill P. G., Tango W. J., Robertson J. G., 2007, MNRAS, 380, 1276
Dobashi K., Uehara H., Kandori R., Sakurai T., Kaiden M., Umemoto T., Sato F., 2005, PASJ, 57, S1
Draine B. T., 2003, ARA&A, 41, 241
Draine B. T., 2009, in Henning Th., Gruen E., Steinacker J., eds, ASP Conf. Ser., Cosmic Dust – Near and Far, in press (arXiv:0903.1658)
Draine B. T., Lee H. M., 1984, ApJ, 285, 89
Draine B. T., Malhotra S., 1993, ApJ, 414, 632
Draine B. T., Allaf-Akbari K., 2006, ApJ, 652, 1318
Draine B. T., Fraisse A. A., 2009, ApJ, 696, 1
Ducati J. R., Bevilacqua C. M., Rembold S. B., Ribeiro D., 2001, ApJ, 558, 309
Fitzpatrick E. L., Massa D. L., 2007, ApJ, 663, 320
Genova R., Beckman J. E., 2003, ApJS, 145, 355
Goodman A. A., Whittet D. C. B., 1995, ApJ, 455, L181
Gordon K. D., Clayton G. C., Smith T. L., Aufdenberg J. P., Drilling J. S., Hanson M. M., Anderson C. M., Mulliss C. L., 1998, AJ, 115, 2665
Greenberg J. M., 1978, in McDonnel J. A. M., ed., Cosmic Dust. John Wiley & Sons, Chichester, p. 187
Greenberg J. M., Li A., 1996, in Block D. L., Greenberg J. M., eds, New Extragalactic Perspectives in the New South Africa. Kluwer, Dordrecht, p. 118
Gupta R., Mukai T., Vaidya D. B., Sen A. K., Okada Y., 2005, A&A, 441, 555
Hanson M. M., Snow T. P., Black J. H., 1992, ApJ, 392, 571
Hildebrand R. H., Dragovan M., 1995, ApJ, 450, 663
Hong S. S., Greenberg J. M., 1980, A&A, 88, 194
Iatì M. A., Saija R., Borghese F., Denti P., Cecchi-Pestellini C., Williams D. A., 2008, MNRAS, 384, 591
Il'in A. E., 1987, Afz, 27, 477
Jones A. P., 2000, J. Geophys. Res., 105, 10257
Kim S. H., Martin P. G., 1994, ApJ, 431, 783
Kim S. H., Martin P. G., 1995, ApJ, 444, 293
Krełowski J., 1989, Astron. Nachrichten, 310, 281
Laor A., Draine B. T., 1993, ApJ, 402, 441
Larson K. A., Whittet D. C. B., 2005, AJ, 623, 897
Lasue J., Levasseur-Regourd A. C., Fray N., Cottin H., 2007, A&A, 473, 641
Lazarian A., 2007, J. Quant. Spectrosc. Radiative Transfer, 106, 225
Lee H. M., Draine B. T., 1985, ApJ, 290, 211
Li A., Greenberg J. M., 1997, A&A, 323, 566
Li A., Greenberg J. M., 1998, A&A, 339, 591
Li A., Greenberg J. M., 2002, ApJ, 577, 789
Li A., Chen J. H., Li M. P., Shi Q. J., Wang Y. J., 2008, MNRAS, 390, L39
Li M. P., Zhao G., Li A., 2007, MNRAS, 382, L26
Mamajek E. E., 2008, Astron. Nachrichten, 329, 10
Martin P. G., 1978, Cosmic Dust. Oxford Univ. Press, Oxford
Martin P. G., 1995, ApJ, 445, L63
Martin P. G., Clayton G. C., Wolff M. J., 1999, ApJ, 510, 905
Mathis J. S., 1986, ApJ, 308, 281
Mathis J. S., 1996, ApJ, 472, 643
Mathis J. S., Rumpl W., Nordsieck K. H., 1977, ApJ, 217, 425
Mermilliod J.-C., Mermilliod M., Hauck B., 1997, A&AS, 124, 349
Min M., Hovenier J. W., Dominik A., de Koter A., Yurkin M. A., 2006, J. Quant. Spectrosc. Radiative Transfer, 97, 161
Monet D. G. et al., 2003, AJ, 125, 984
Moreno F., Muñoz O., Guirado D., Vilaplana R., 2007, J. Quant. Spectrosc. Radiative Transfer, 106, 348
North J. R., Davis J., Tuthill P. G., Tango W. J., Robertson J. G., 2007, MNRAS, 380, 1276
Onaka T., 1980, Ann. Tokyo Astron. Obser., 18, 1
Penprase B. E., Blades J. C., Danks A. C., Crane P., 1990, ApJ, 365, 241
Platais I., Kozhurina-Platais V., van Leeuwen F., 1998, AJ, 116, 2423
Rogers C., Martin P. G., 1979, ApJ, 228, 450
Rouleau F., Martin P. G., 1991, ApJ, 377, 526
Serkowski K., Robertson J. W., 1969, ApJ, 158, 441
Skiff B. A., 2009, Catalogue of Stellar Spectral Classifications, Lowell Obs. VizieR On-line Data Catalog
Snow T. P., McCall B. J., 2006, ARA&A, 44, 367
Snow T. P., Destree J. D., Welty D. E., 2006, ApJ, 679, 512
Sofia U. J. et al., 2005, ApJ, 625, 167

Stark C. R., Potts H. E., Diver D. A., 2006, A&A, 457, 365
Straizys V., 1992, Multicolor Stellar Photometry. Pachart Publ. House, Tucson
Vaidya D. B., Gupta R., Dobbie J. S., Chỳlek P., 2001, A&A, 375, 584
Vallée J. P., 2004, New Astron. Rev., 48, 763
Vallée J. P., 2008, ApJ, 681, 303
Valencic L. A., Clayton G. C., Gordon K. D., 2004, ApJ, 616, 912
Voshchinnikov N. V., 1989, Astron. Nachrichten, 310, 265
Voshchinnikov N. V., 2004, Astrophys. Space Phys. Rev., 12, 1
Voshchinnikov N. V., Farafonov V. G., 1993, Ap&SS, 204, 19
Voshchinnikov N. V., Il'in V. B., 1993, SvA, 37, 21
Voshchinnikov N. V., Farafonov V. G., 2003, J. Comput. Math. Math. Phys., 43, 1299
Voshchinnikov N. V., Das H. K., 2008, J. Quant. Spectrosc. Radiative Transfer, 109, 1527 (VD08)
Voshchinnikov N. V., Il'in V. B., Henning Th., Dubkova D. N., 2006, A&A, 445, 167
Wegner W., 2002, Baltic Astron., 11, 1
Weingartner J. C., Draine B. T., 2001, ApJ, 548, 296
Welsh B. Y., Sallmen S., Jelinsky S., 2005, A&A, 440, 547
Whittet D. C. B., 2003, Dust in the Galactic Environment. IOP, Bristol
Wilking B. A., Lebofsky M. J., Martin P. G., Rieke G. H., Kemp J. C., 1980, ApJ, 235, 905
Wilking B. A., Lebofsky M. J., Rieke G. H., 1982, AJ, 87, 695
Wolf S., Voshchinnikov N. V., Henning Th., 2002, A&A, 385, 365
Zubko V. G., Krełowski J., Wegner W., 1996, MNRAS, 283, 577
Zubko V. G., Krełowski J., Wegner W., 1998, MNRAS, 294, 548

This paper has been typeset from a TEX/LATEX file prepared by the author.